Interim Status Report

on

Research on Miniature Gas Analysis Systems
NGR 05-020-690

Submitted to

National Aeronautics and Space Administration

by

James B. Angell
Electrical Engineering Department
Stanford University

2 January 1974

Research on Miniature Gas Analysis Systems

I. Introduction

This report is intended to describe the research work that was conducted during the period from September through December 1973 on grant number NGR 04-020-690 in the Integrated Circuits Laboratory of the Stanford Electronics Laboratories in Stanford University. The majority of the work during this period was concentrated on the technology for fabricating very small valves, whose function will be to introduce a small sample of the gas to be analyzed into the main carrier gas stream flowing through the chromatograph column. In addition, some analyses have been made of the factors governing the resolution of gas chromatographs, particularly those with miniature columns. These anlayses showed how important the column lining thickness is in governing the ability of a miniature column to separate components of an unknown gas. A brief description of column lining factors is included herewith. Finally, preliminary work on a super small thermistor detector was performed. This work showed the importance of having the thermistor as small as possible, and led to the suggestion that intrinsic silicon may be ideal for this application. To this end, some 10,000 ohm-cm silicon has been obtained. The following sections describe work on each of these areas in greater detail.

II. Miniature Valves

The small volume and low flow rates used in a miniature gas chromatography system require that the injected sample, and indeed the complete valving system, be of extremely small volume. The integrated circuit techniques of silicon etching and bonding make it feasible to integrate a micro-volume sample valving and injection system on the same wafer as the column. The small size of the valves and connecting capillaries, and the close proximity of the valving system to the column eliminate much of the "dead volume" and sample diffusion associated with standard valves and connecting tubing.

The miniature valves developed for the injection system are gas actuated, ON-OFF, diaphragm valves. When control pressure is applied to the valve, a flexible silicon diaphragm is held against a silicon seat, shutting off the gas flow. The diaphragm valve is sandwiched between a silicon wafer and its glass cover plate, and is completely compatible with miniature GC column fabrication.

Two possible sample injection schemes utilizing miniature valves are shown in figure 1. The 5-valve system uses ON-OFF valves in a configuration similar to that used in large chromatography systems. The carrier gas is normally directed into the column, while the sample gas is collected in a chamber of known volume. To inject the sample, all five valves change state simultaneously. The carrier gas is rerouted through the sample chamber, sweeping the sample as a "plug" into the column. The advantage of this system is that the volume of the sample is determined solely by the volume of the sample chamber and not by the speed of operation of the valves. The main drawback of this system lies in the fact that five valves have to be fabricated on the same wafer as the column. This leads to greatly increased fabrication problems and a correspondingly low yield. For this reason, the simpler 2-valve system is currently being developed for use in the miniature chromatograph.

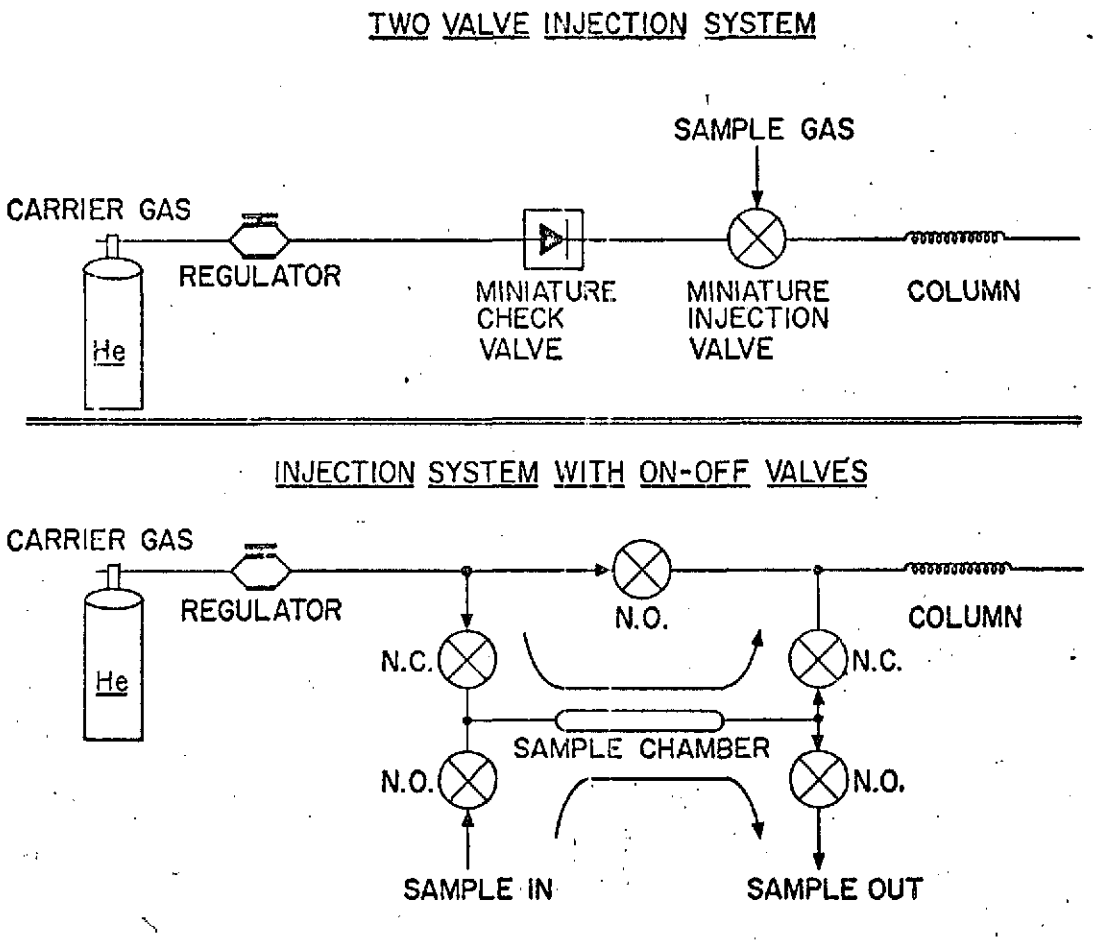

Figure 1

Two possible injection schemes utilizing miniature valves.

The 2-valve system consists of an injection valve and a check valve. Carrier gas normally flows through the injection valve and into the column. When the injection valve is opened, high pressure sample gas flows into the carrier gas capillary. The check valve prevents the sample plug from travelling upstream towards the carrier gas supply. The amount of sample introduced is dependent upon the sample pressure and the length of time that the injection valve is open.

Valve Construction

Figure 2 shows an exploded view and a cross section of the miniature ON-OFF valve. A 2 mm diameter well is etched into a silicon wafer to form the valve cavity. Since the bottom of this well will serve as the valve seat, HF-HNO_3 is used as the etchant to provide a flat, polished surface. The depth of the well has to be between 55 and 60 microns to accommodate the diaphragm structure while restricting the diaphragm to a maximum downward defelction of 10 microns. A subsequent photolithography is used to define a ring of 400-microns outside diameter and 40-micron annular thickness in the center of the valve well. A second HF-HNO_3 etch is used to etch the bottom of the valve well 10 microns deeper everywhere except under the ring. The result is a raised silicon ring protruding 10 microns above the bottom surface of the valve well. It is this silicon ring which forms the seat for the diaphragm valve.

In another photolithography and etch step, the trench for the output gas capillary is etched from the lip of the valve well, across the wafer to an output port. Using an anisotropic etchant (KOH), a hole is then etched from the backside, through the wafer to the center of the valve well. The dimensions of this orifice are determined by the backside etch mask and the thickness of the silicon wafer. In the current valve design, the orifice is approximately 130 microns square. Figures 3 and 4 are photographs of the etched valve well, seating ring, and orifice.

The valve diaphragm is a silicon disk 1.6 mm in diameter and approximately 8 microns thick. A 50 micron thick guard ring around the outside of the diaphragm provides support for mounting. Silicon was chosen for the diaphragm material because the anodic bonding process requires temperatures in excess of 300 °C, and the thermal expansion coefficients of all the materials used have to be well matched to that of the silicon wafer. The diaphragm is fabricated using an anisotropic etchant and a previously developed technique for controlling the diaphragm thickness. A pressure differential of 8 psi on opposite sides of the diaphragm results in a center deflection of approximately 25 microns. A 25 psi differential is sufficient to rupture the diaphragm.

The glass cover plate which is anodically bonded to the silicon wafer is type 7740 pyrex glass of 125 microns thickness. The glass is polished optically flat on the surface to be bonded to the silicon wafer. A 0.2-mm hole is etched through the glass for the control pressure port. The guard ring on the silicon diaphragm is then centered beneath the control port and is anodically bonded to the pyrex. The bonding process forms a hermetic seal which prevents any of the control gas from leaking into the valve. With the diaphragm centered over the valve seat, the glass cover plate is anodically bonded to the siiicon wafer. Figure 5 is a photograph of the valve taken through the cover glass. The dark area in the center of the diaphragm are the sides of the control port hole. The valve orifice and seating ring are covered by the diaphragm.

EXPLODED VIEW OF MINIATURE VALVE

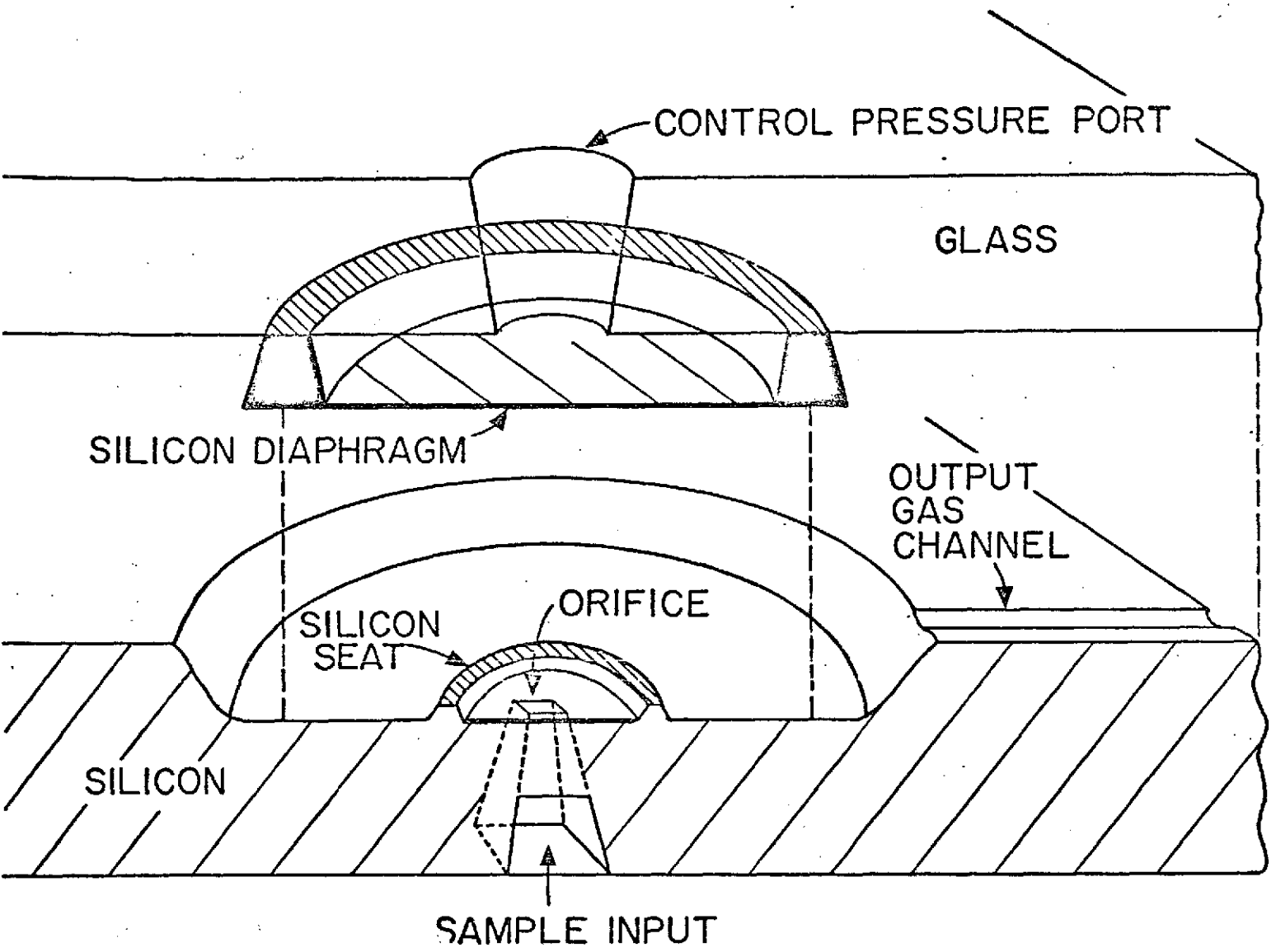

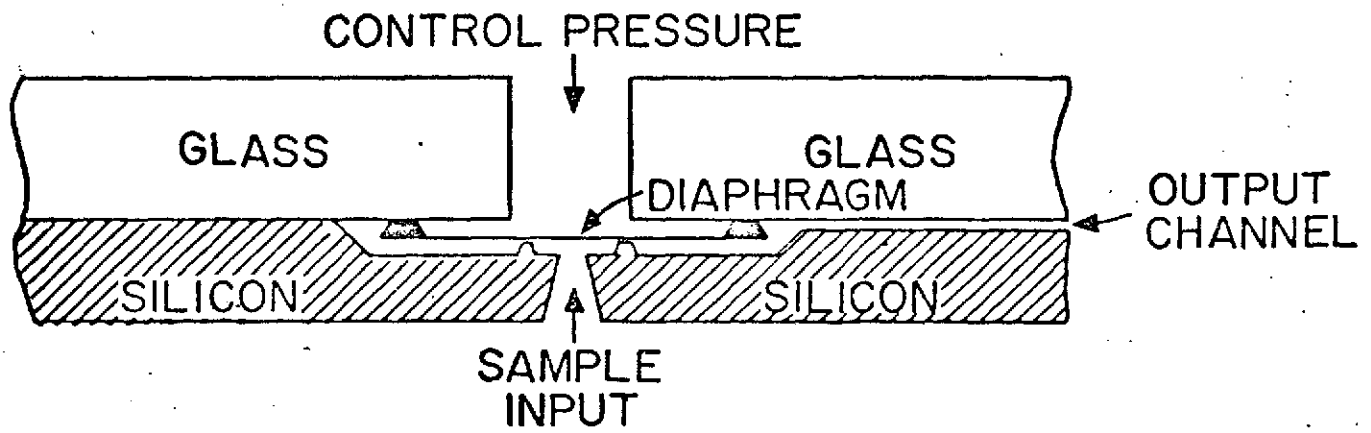

CROSS SECTION OF VALVE

Figure 2

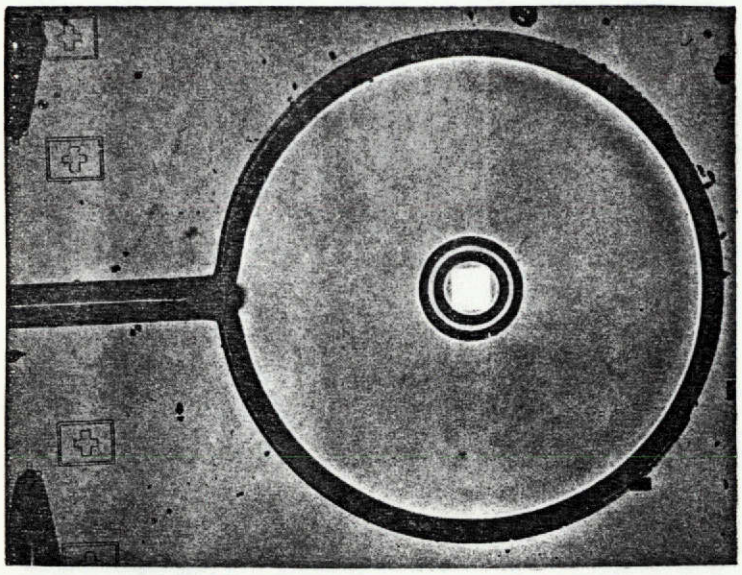

FIGURE 3 -- Photograph of etched valve well, seating ring, and orifice. Magnification 31 X

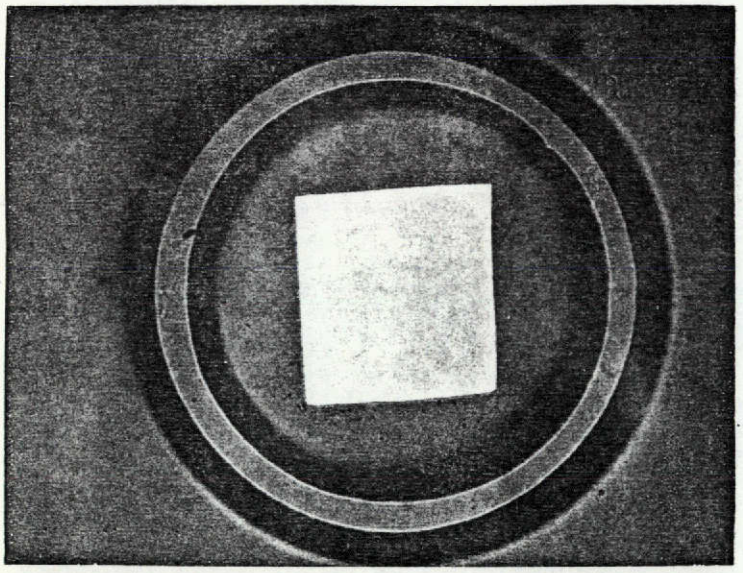

FIGURE 4 -- Photograph of seating ring and orifice. Magnification 150 X

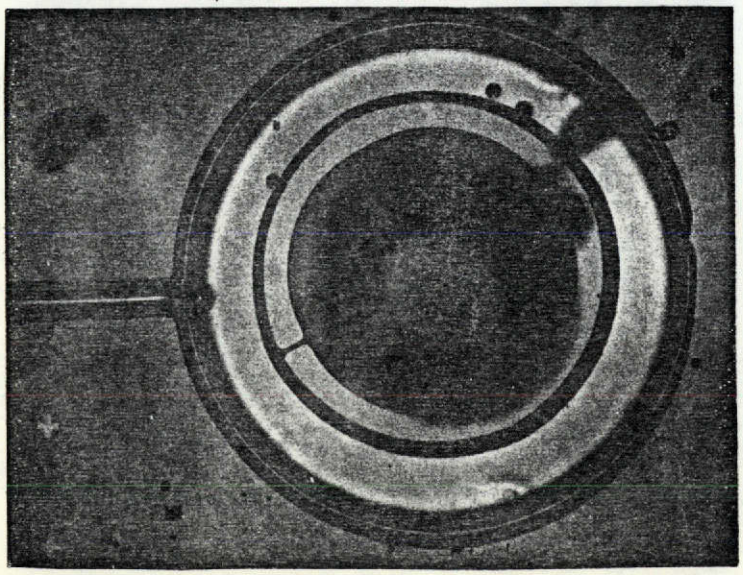

FIGURE 5 --Photograph of complete valve looking through glass cover plate. Magnification 31 X

The construction of the miniature check valve is similar to that of the ON-OFF valve except in two respects. First, the seating ring is recessed only 40 microns below the top surface of the silicon wafer. This results in the diaphragm being normally deflected 10 microns by the seating ring. Sufficient force is exerted by diaphragm tension to seal off any gas flow. The control pressure port is also absent. Instead, the backside of the diaphragm is vented to the output side of the valve (the valve well). Gas flow in the forward direction results if the input pressure is sufficient to overcome the diaphragm tension and unseat the valve. Reverse flow is prevented, since having an output pressure greater than the input pressure will force the diaphragm against the seat.

Evaluation of Valves

ON-OFF valves have been fabricated and their operation tested. With approximately 9 micron thick diaphragms, they exhibit complete gas shutoff when the applied control pressure is at least 6 psi greater than the input pressure. The diaphragm seal to the pyrex glass is reproducibly hermetic, and no control gas has been observed leaking into the valve. Speed of operation appears to be limited only by the switching speed of the control pressure: approximately 10 ms. Lifetime and maximum pressure ratings of the valves have yet to be determined.

The check valves which have been fabricated have only been partially evaluated. The most common failure is incomplete seating of the diaphragm, resulting in gas flow in the reverse direction. This is caused by irregularities in the height of the silicon seating ring. Those valves which do work exhibit no reverse gas flow, and forward flow only for input pressures above a certain threshold. This threshold pressure varies from 8 to 40 psi depending on the height of the seating ring. These valves have yet to be tested with greater than one atmosphere output pressures. This situation will occur when the valve is used in conjunction with the miniature column.

Integration of Valves and Column

Figure 6 shows the cross section of the two valve injection system as it will be fabricated on the same wafer as the spiral capillary column. The ON-OFF valve is constructed on the backside of the wafer to minimize the dead volume of the valve as seen by the carrier gas capillary. This dead volume is the etched orifice. It is approximately 1.5 nanoliters with the current valve design. The two-sided geometry also eliminates the problem of having to etch a control pressure port for the ON-OFF valve through the thick glass on the column side of the wafer.

It is hoped that with this design, sufficiently small samples can be injected directly into the column without having to use a sample splitter. However, if a sample splitter proves to be necessary, it too can be integrated onto the wafer between the valving system and the column.

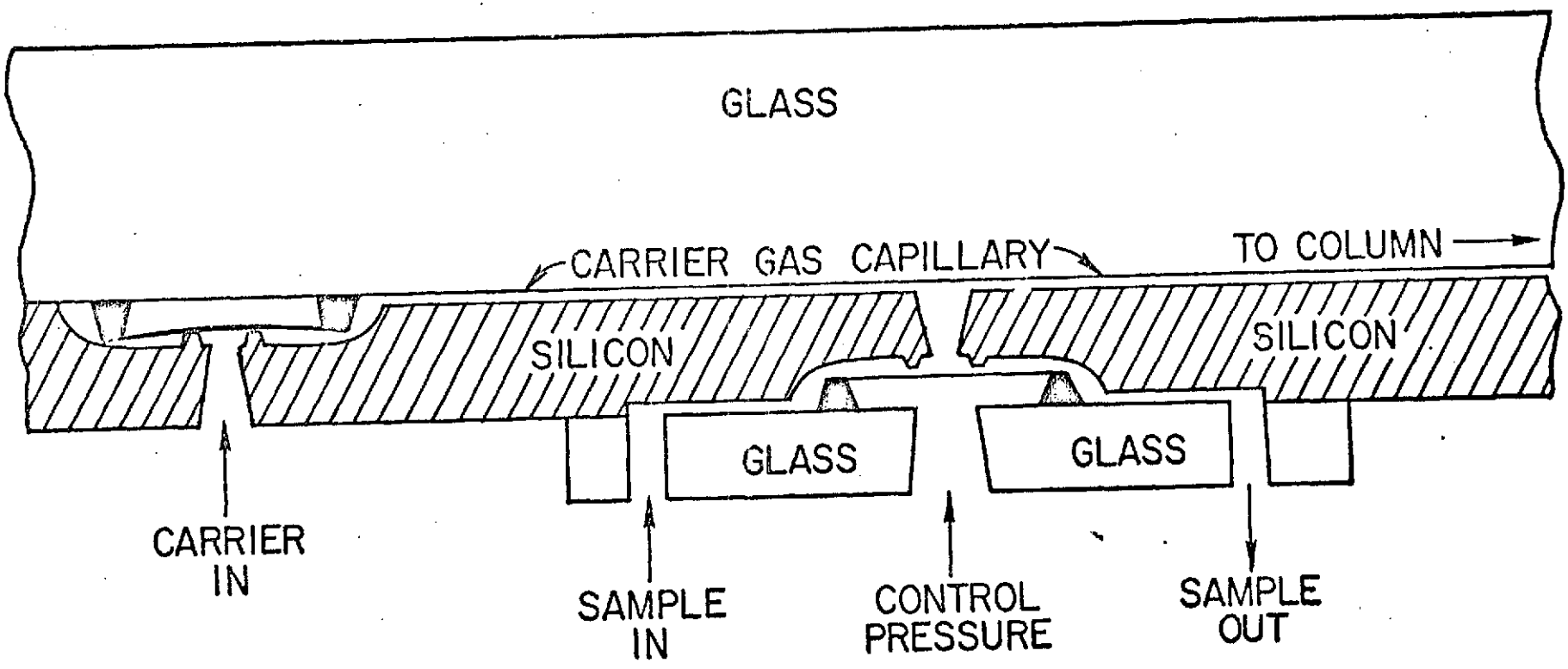

CROSS SECTION OF 2 VALVE INJECTION SYSTEM

Figure 6

III. Theory of Gas Chromatographs with Miniature Columns

One of the classical measures of column efficiency is the plate height of the column. This characterizing parameter was originally associated with the length of imagined equilibration stages in the column. However, since the equilibration stages model provides a misleading picture of column operation, it has been abandoned; but the plate height parameter retained. It is now defined as

$$H = \frac{d\sigma_{\ell}^2}{dL} \qquad (1)$$

ie. the increase in peak variance per unit column length. In a uniform column of length L in a constant environment, equation 1 becomes:

$$H = \frac{\sigma_{\ell}^2}{L} \qquad (2a)$$

Expressed in terms of eluted gas volume,

$$H = L\left(\frac{\sigma}{V_R'}\right)^2 \qquad (2b)$$

As depicted in figure 7, V_R' is the volume of gas eluted, from the time the sample was injected to the time that the center of the peak emerged from the column. σ is the standard deviation of the ideal gaussian output expressed in the same units as V_R'.

The number of theoretical plates contained in the column is expressed as:

$$N = L/H = \left(\frac{V_R'}{\sigma}\right)^2 \qquad (3)$$

Instead of the standard deviation σ, the basewidth of the gaussian peak $w = 4\sigma$ is typically used in the plate equations. Therefore,

$$N = 16\left(\frac{V_R'}{w}\right)^2 \qquad (4)$$

The measured retention volumn V_R' can be broken into two components, $V_R' = V_d + V_R$. V_d is the volume of gas in the column, injection, and detection systems. It is determined by the geometry of the system and equals the retention volume of an unretained gas such as air. V_R is the true retention volume. It is the result of the retarding interaction between the sample and the liquid phase.

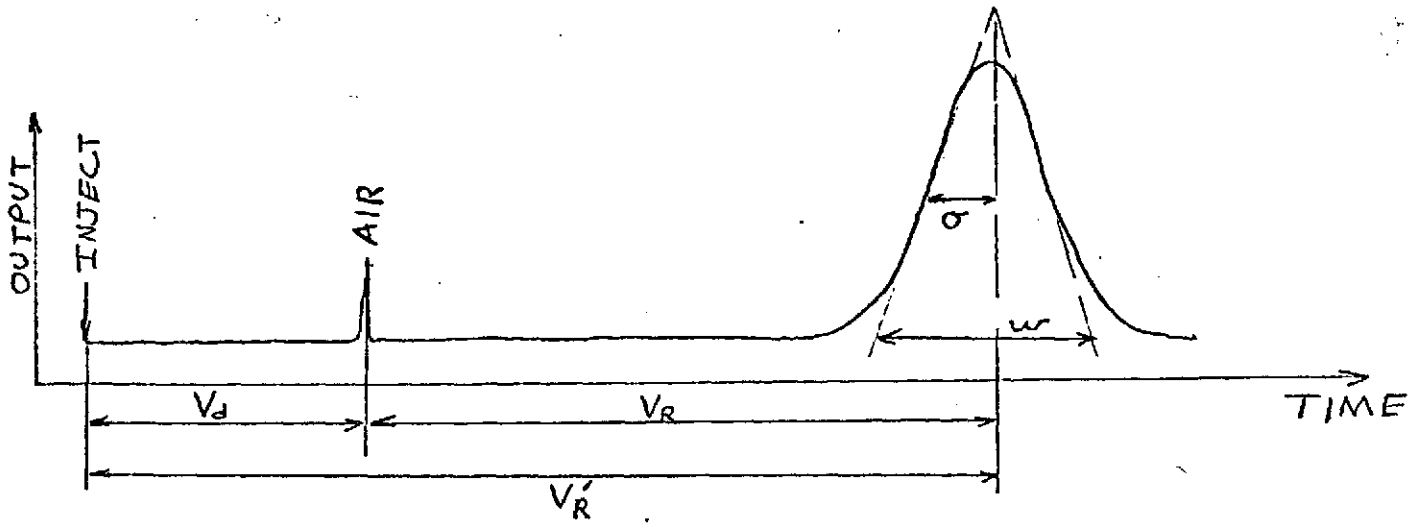

Figure 7. Typical GC Output

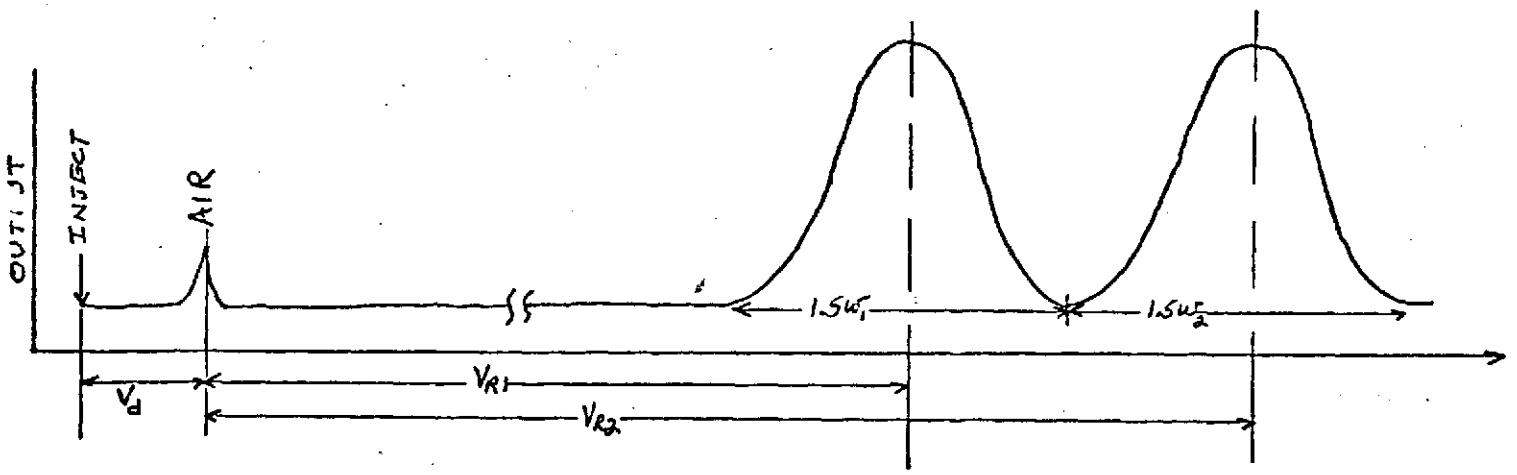

Figure 8. GC Output - Two Peaks Just Separated

The number of plates in the column,

$$N = 16\left(\frac{V_d + V_R}{w}\right)^2 \qquad (5)$$

can be viewed as a measure of efficiency since it relates the amount of peak distortion (spreading) to the length of time that the sample was in the column. What N does not measure, however, is the separation of two sample components achieved by the column. It has been shown[1] that as V_R is decreased by changing the amount of stationary phase in a column, the number of plates needed to just separate two sample peaks increases. However, the ratio V_R/w remains constant close up for all cases in which the two peaks have the same degree of separation. For this reason a separation factor S has been defined as:

$$S = 16\left(\frac{V_R}{w}\right)^2 \qquad (6)$$

Assuming that a gaussian peak has a width of $6\sigma = 1.5w$, figure 8, then two peaks with respective true retention volumes and widths V_{R1}, V_{R2}, w_1, w_2 are just separated when

$$1.5\left(\frac{w_1 + w_2}{2}\right) = V_{R2} - V_{R1} \qquad (7)$$

Assuming further that $w_1 = w_2$, a reasonable assumption for peaks that are very close together, then

$$w = \frac{1}{1.5}\left(V_{R2} - V_{R1}\right) \qquad (8)$$

Substituting into equation 6 yields:

$$S = 36\left[\frac{V_{R2}}{V_{R2} - V_{R1}}\right]^2 \qquad (9)$$

For two solutes with relative volatilities $\alpha = V_{R2}/V_{R1}$, the separation factor (eqn. 9) needed to just separate their output peak is:

$$S = 36\left(\frac{\alpha}{\alpha - 1}\right)^2 \qquad (10)$$

Any column with that value of S, regardless of the number of plates it contains, will just separate those two solutes.

The partition ratio k, the ratio of the amount of solute in the liquid phase in equilibrium to the amount is the gas phase, is related to the retention volume by:

$$k = \frac{V_R}{V_d}$$

Using this relation and equations 5 and 6, the separation factor can be related to the number of plates in the column by:

---

[1] Purnell, Journal of Chemical Society 1960, p 1268

$$N = S\left(\frac{k + 1}{R}\right)^2 \qquad (11)$$

or in terms of plate height,

$$1/S = \left(\frac{k + 1}{R}\right)^2 \frac{H}{L} \qquad (12)$$

The plate height of an open tubular capillary column has been related to the column parameters by Golay[2] as:

$$H = \frac{2D_g}{u} + \left\{\frac{1 + 6k + 11\,k^2}{24(1 + k)^2}\ \frac{r^2}{D_g} + \frac{2}{3}\ \frac{k}{(1 + k)^2}\ \frac{d^2}{D_l}\right\} u \qquad (13)$$

where: r = column radius
u = average carrier gas velocity
L = column length
k = partition ratio
d = thickness of stationary phase layer coating the column
D_g = diffusion coefficient of the solute in the carrier gas
D_l = diffusion coefficient of the solute in the stationary phase

Substituting into equation 12 yields S expressed as a function of column parameters.

$$1/S = \left(\frac{1 + k}{k}\right)^2 \frac{2D_g}{uL} + \left\{\frac{1 + 6k + 11k^2}{24k^2 D_g} + \frac{2}{3}\ \frac{1}{k}\ \frac{d^2}{r^2}\right\} \frac{ur^2}{L} \qquad (14)$$

Since the above equation can be optimized with respect to carrier gas velocity u, it can be assumed that the column is operated at the optimum velocity, for which we have:

$$1/S = \frac{2r}{L}\left(\frac{1 + k}{k}\right)\left(\frac{1 + 6k + 11k^2}{12k^2} + \frac{4}{3}\ \frac{1}{k}\ \frac{d^2}{r^2}\ \frac{D_g}{D_l}\right)^{1/2} \qquad (15)$$

The partition ratio k used in the above equations is a function of column radius. It is related to a more fundamental parameter, the partition coefficient K, by the equation

$$k = \frac{2dK}{r} \qquad (16)$$

The partition coefficient K is defined as the concentration of solute in the stationary phase divided by the concentration of solute in the gas phase. It is only a function of the thermodynamic properties of the solute and the stationary phase.

For limited ranges of temperature, the partition coefficient is approximated by

$$K = ce^{\Delta H_s/RT}$$

---

[2] Golay, M.J., "Gas Chromatography, 1958," D. H. Desty, ed., p. 36, Academic Press, New York, 1958.

where c = constant
R = universal gas constant
T = temperature
ΔH_s = heat of solution of solute in stationary phase

The exponential dependence upon temperature makes K the most temperature dependent parameter and facilitates the control of column performance with simple temperature adjustments.

Figure 9 is a plot of separation factor S (equation 15) as a function of column radius. The partition coefficient K is varied as a parameter. The other column parameters were held constant at their nominal values:

$L = 100$ cm
$d = .5\ \mu$
$D_g = .1\ cm^2/sec$
$D_l = 10^{-6}\ cm^2/sec$

Figure 10 is a plot of the optimum carrier velocity as a function of radius. A slight variation with partition coefficient K is observed.

The pressure drop across the column for a given flow rate is given by Poiseuilles equation

$$\Delta P = \frac{U8\eta L}{r^2} \tag{17}$$

where η is the viscosity of the carrier gas. Figure 11 is a plot of log pressure drop versus radius for optimum flow rates of helium carrier gas.

Resistance to Mass Transfer

The separation factor with optimized carrier velocity can be expressed in a simplified form as

$$1/S = \left(\frac{k+1}{k}\right)^2 \left(B\left[C_L + C_g\right]\right)^{1/2} \tag{18}$$

$$B = 2D_g$$

$$C_l = 2/3\ \frac{k}{(1+k)^2}\left(\frac{d^2}{D_L}\right)$$

$$C_g = \frac{1 + Gk + 11k^2}{24\ (1+k)^2}\ \left(\frac{r^2}{D_g}\right)$$

The C_g and C_l terms can be regarded as the resistance to mass transfer of the solute in the mobile and stationary phases respectively. They represent the departure from the ideal condition of instantaneous equilibrium between the solute in the mobile and stationary phases.

Figure 12 is a plot of the relative magnitudes of C_l and C_g as a function of K. Column radius is varied as a parameter. The separation of sample constituents with light molecules (low values of K) is dominated by C_l term, especially in columns of very small radii. Figure 13 shows that for a fixed radius, the value of the dominant C_l term can be lowered by decreasing the stationary phase thickness.

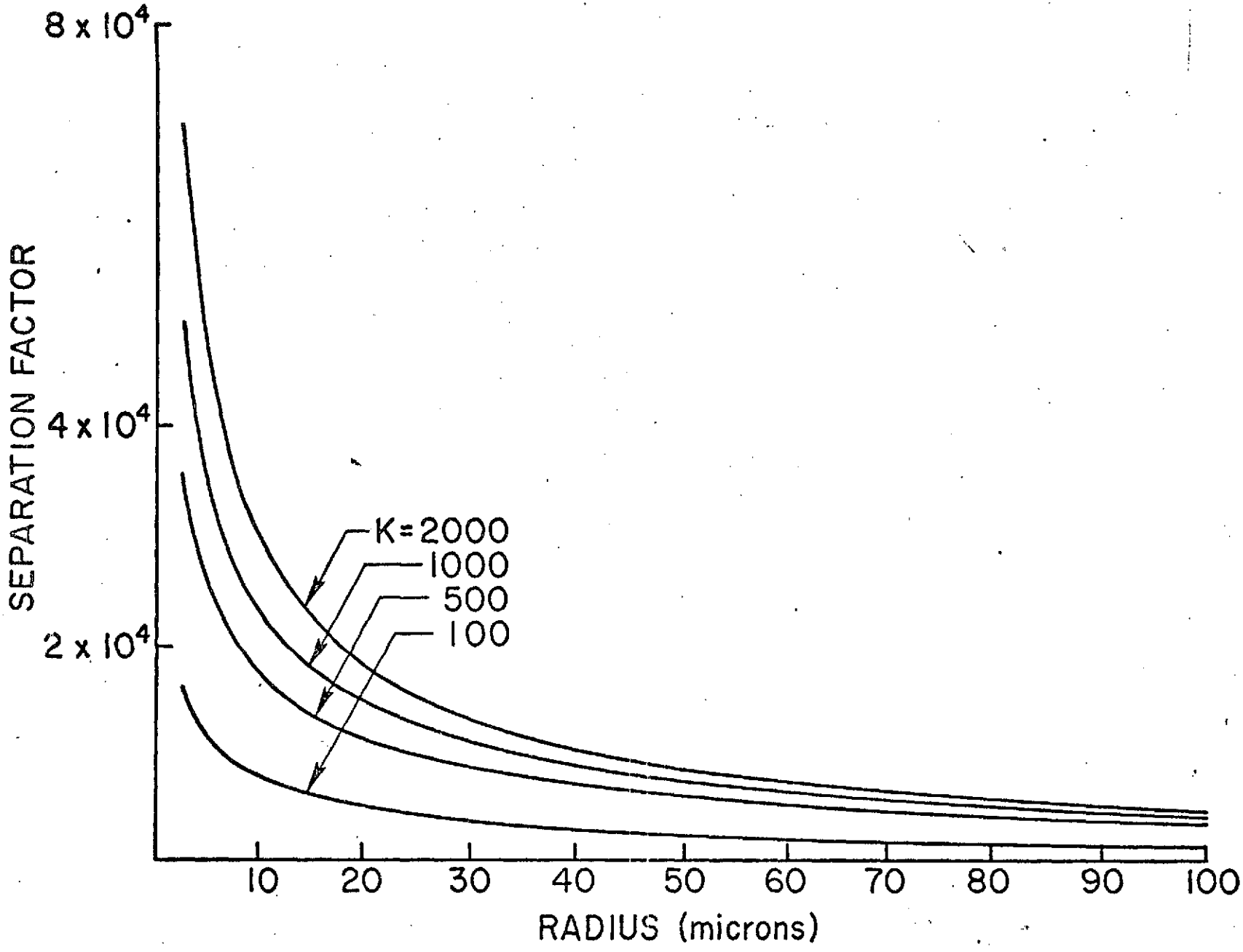

Figure 9

Plot of separation factor S as a function of column radius.

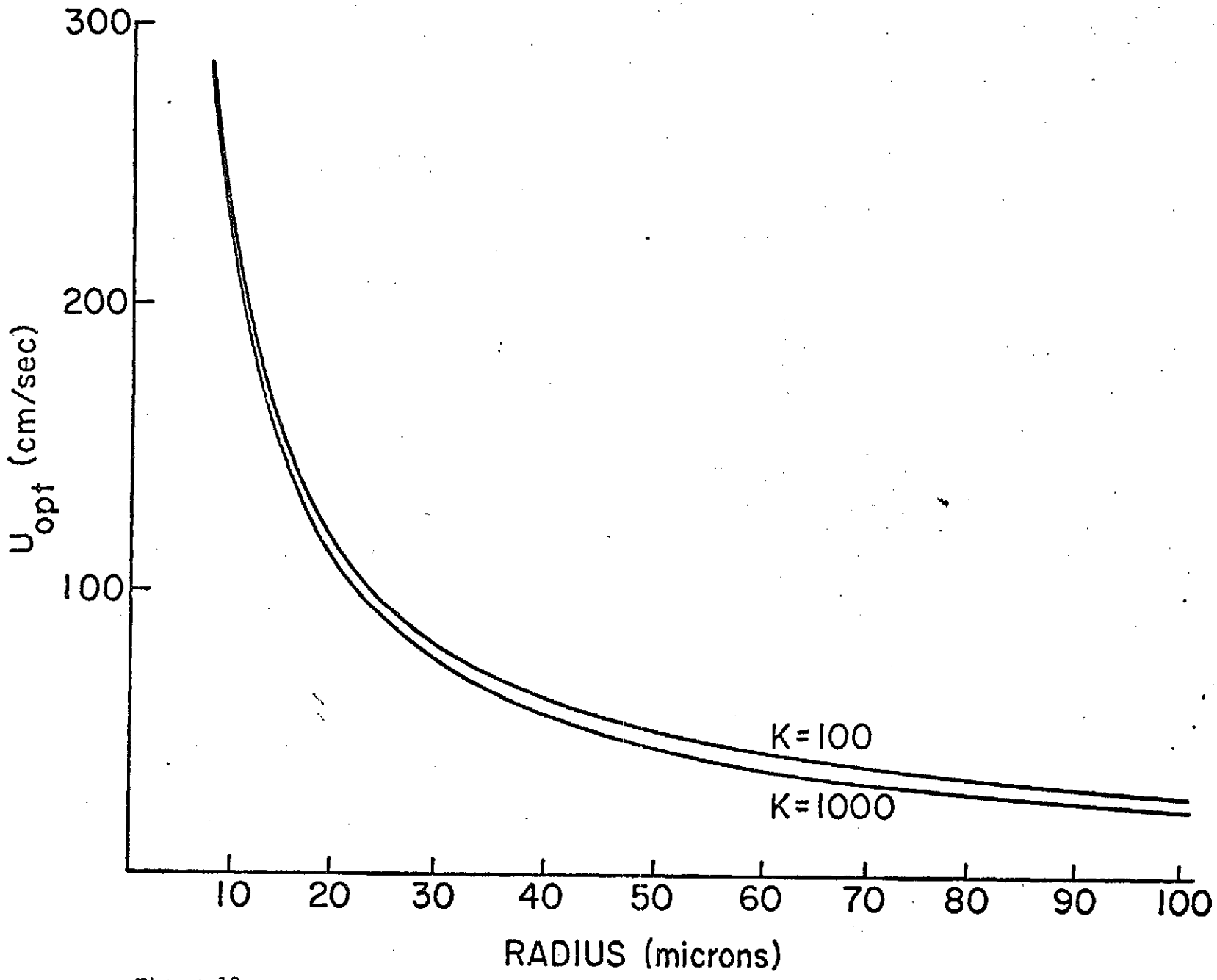

Figure 10
A plot of the optimum carrier velocity as a function of radius.

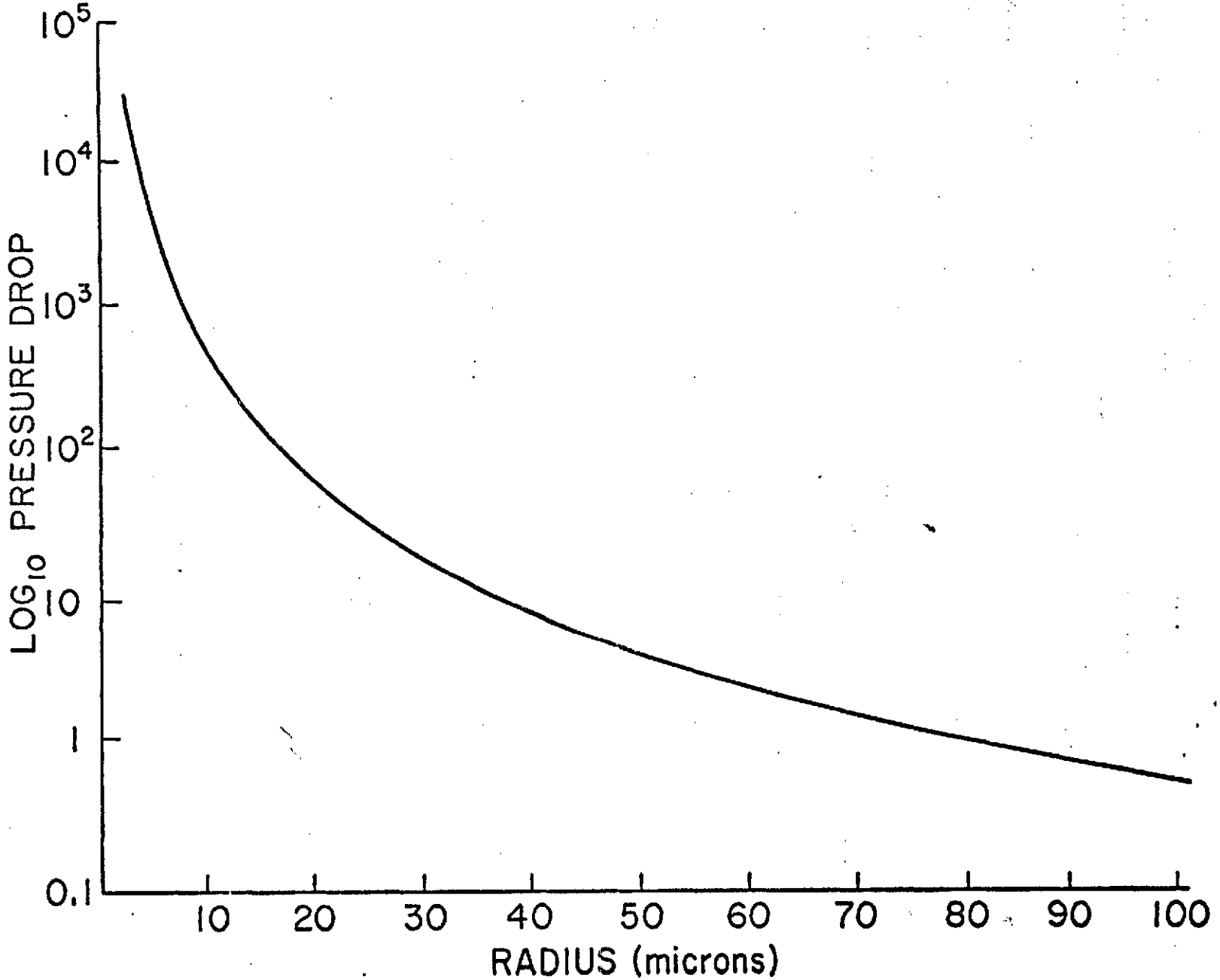

Figure 11

A plot of log pressure drop versus radius for optimum flow rates of helium carrier gas.

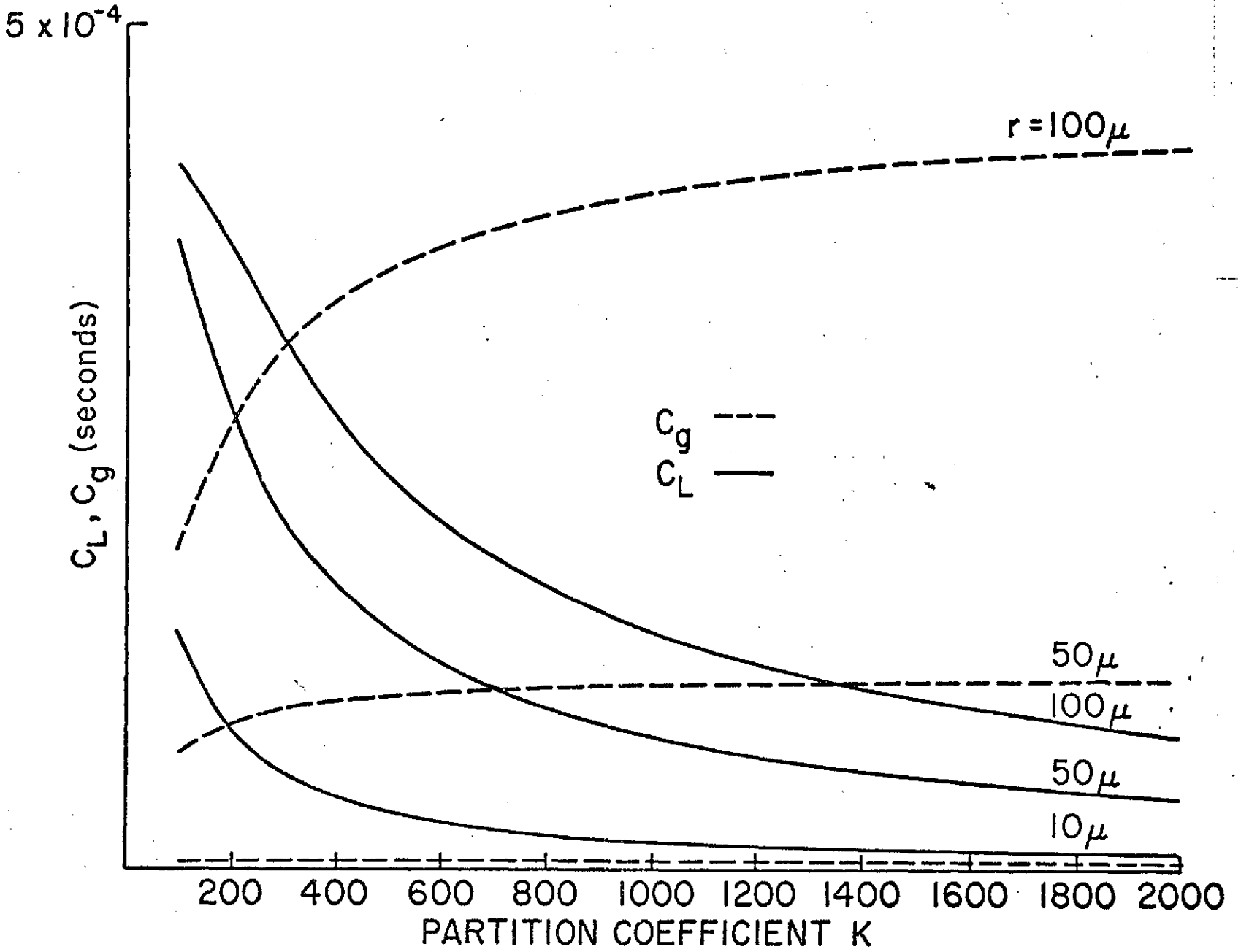

Figure 12
A plot of the relative magnitudes of C_l and C_g as a function of K.

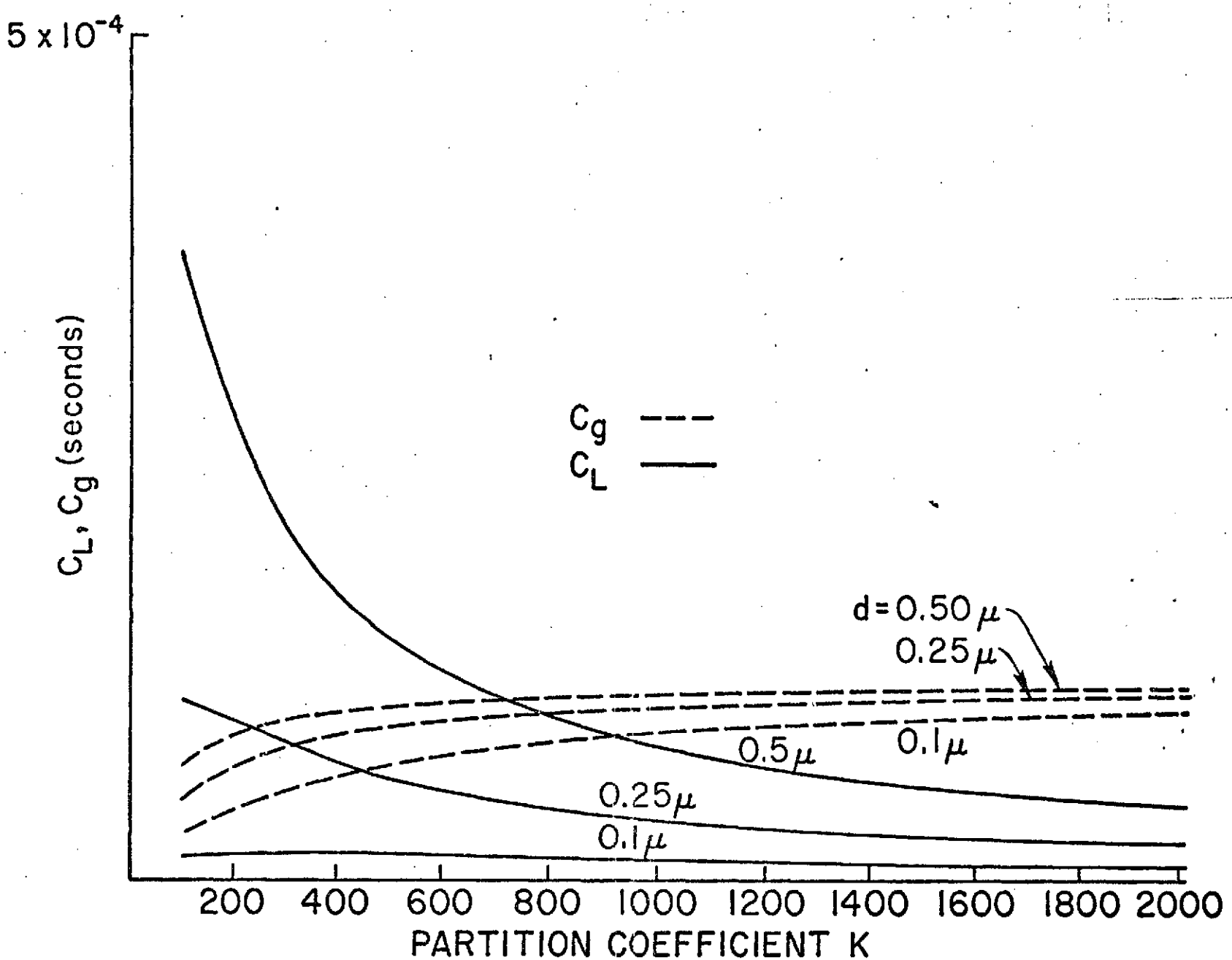

Figure 13

Shows that for a fixed radius, the value of the dominant C_l term can be lowered by decreasing the stationary phase thickness.

Figure 14 is a plot of C_l and C_g as a function of column radius. The partition coefficient K is varied as a parameter.

Miniature GC Columns

As shown in Figure 9, the separation factor exhibits a 1/r dependence for values of r less than 50 μ. For radii less than 20 μ, S increases very rapidly as the radius decreases. It is in this range of small radii and high separation factors that the miniature capillary columns will operate. Since S is directly proportional to column length, the increased S due to the small radius is necessary to compensate for the very short column length. Figure 4 and 6 and Equation 18 indicate that the decrease in C_l and C_g with decreasing radius is responsible for the increase in separation.

The price to be paid for decreasing the capillary radius is the pressure drop across the column needed to maintain optimum carrier velocity, Figure 5. Assuming a maximum pressure drop of 100 psi, the minimum radius for which flow can be optimized is 17.5 μ. For radii less than that, there will be a sharp decrease in separation due to non-optimum carrier velocity.

An informative approach to the problem is to set a maximum pressure drop, and determine the resulting separation factor as a function of column radius. Using Equations 14 and 17, S as a function of r is plotted in Figure 15. The pressure drop p is varied as a parameter. For each value of p, the corresponding curve peaks at the radius for which the carrier velocity is optimized.

As the parameters in Equation 14 are varied, the height and position of each Δp curve in Figure 15 change. Figure 16 shows how the $p = 10$ psi curve varies with column length. This figure indicates that for radii greater than 15 μ, greater separation can be achieved by increasing column length.

Figure 17 is a plot of separation with $p = 10$ and K as a parameter. Since the curves in Figure 17 peak at different values of radius as K is varied, the column radius should be optimized for the sample with the smallest value of K. This gives the best separation of the hardest to separate pair of solutes.

Figures 18 and 19 show the variation of separation as D_g (the diffusion coefficient of the solute in the carrier gas) and d (the stationary layer thickness) are varied. It is evident from these plots that the gas phase diffusion process is dominant in columns with radii less than 30 μ. D_g can be decreased by using a heavier carrier such as CO_2 or N_2.

The "typical" values of the parameters used in plotting the separation factor curves are typical of GC systems in general, but they may be unattainable in the miniature system. The stationary phase thickness d is especially critical. The model used by Golay in developing the equations for H assumes a uniform thickness d. This is in itself unattainable since capillary forces tend to draw the liquid into pools. This situation is even more exaggerated in the miniature column since the capillary is not of circular cross section. The range of liquid layer thicknesses attainable and their uniformity in the miniature columns have yet to be determined.

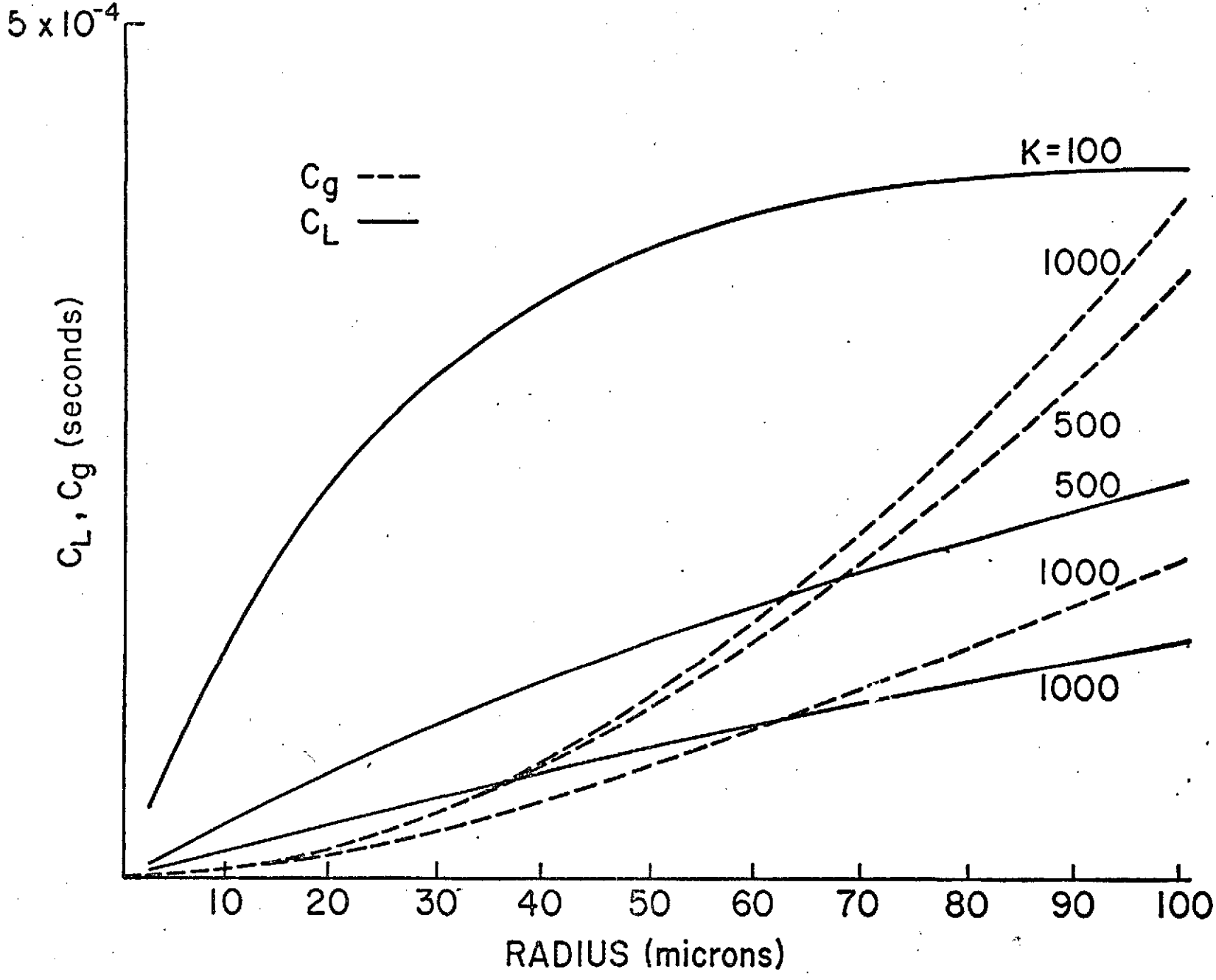

Figure 14
A Plot of C_l and C_g as a function of column radius.

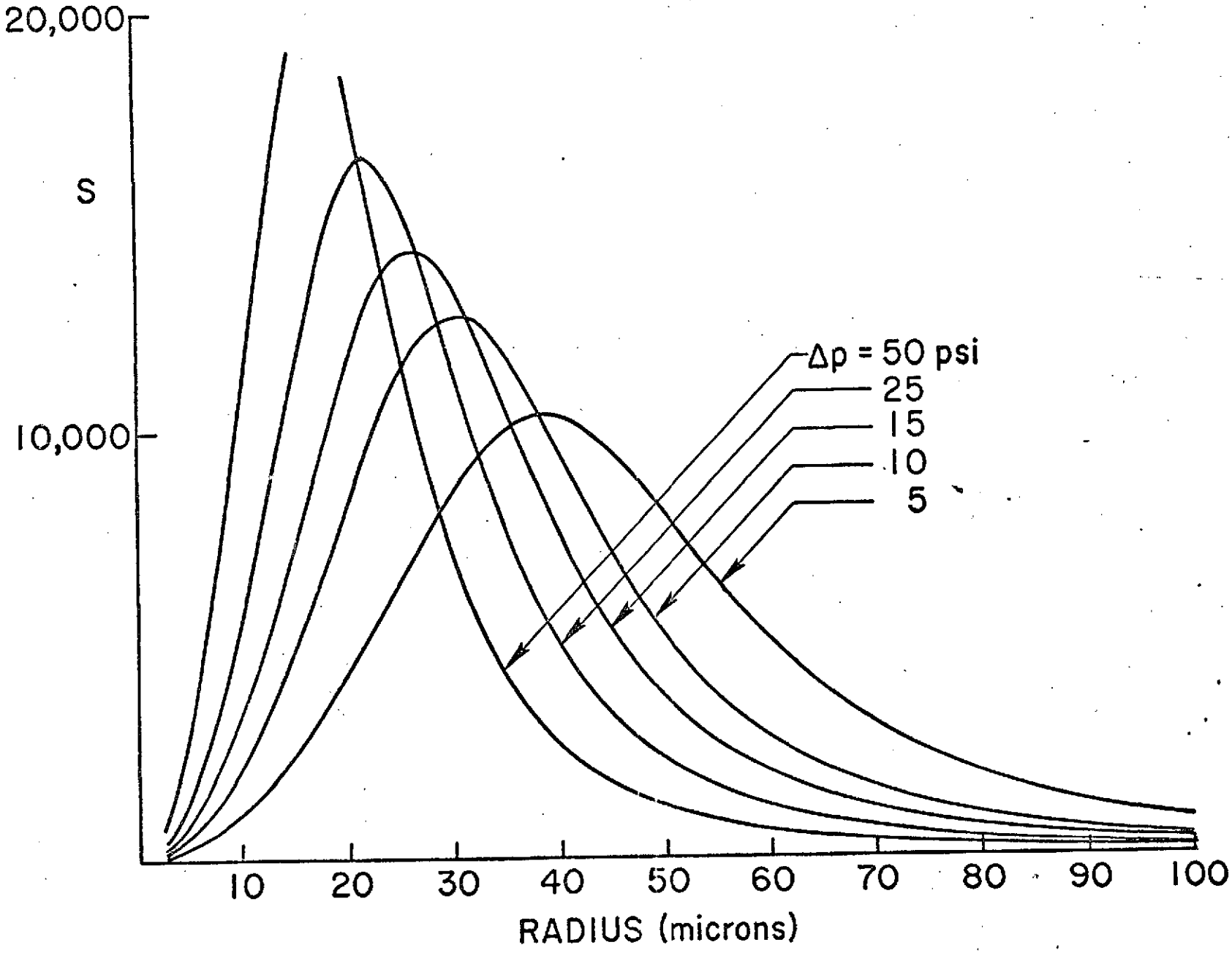

Figure 15
Change of Δp.

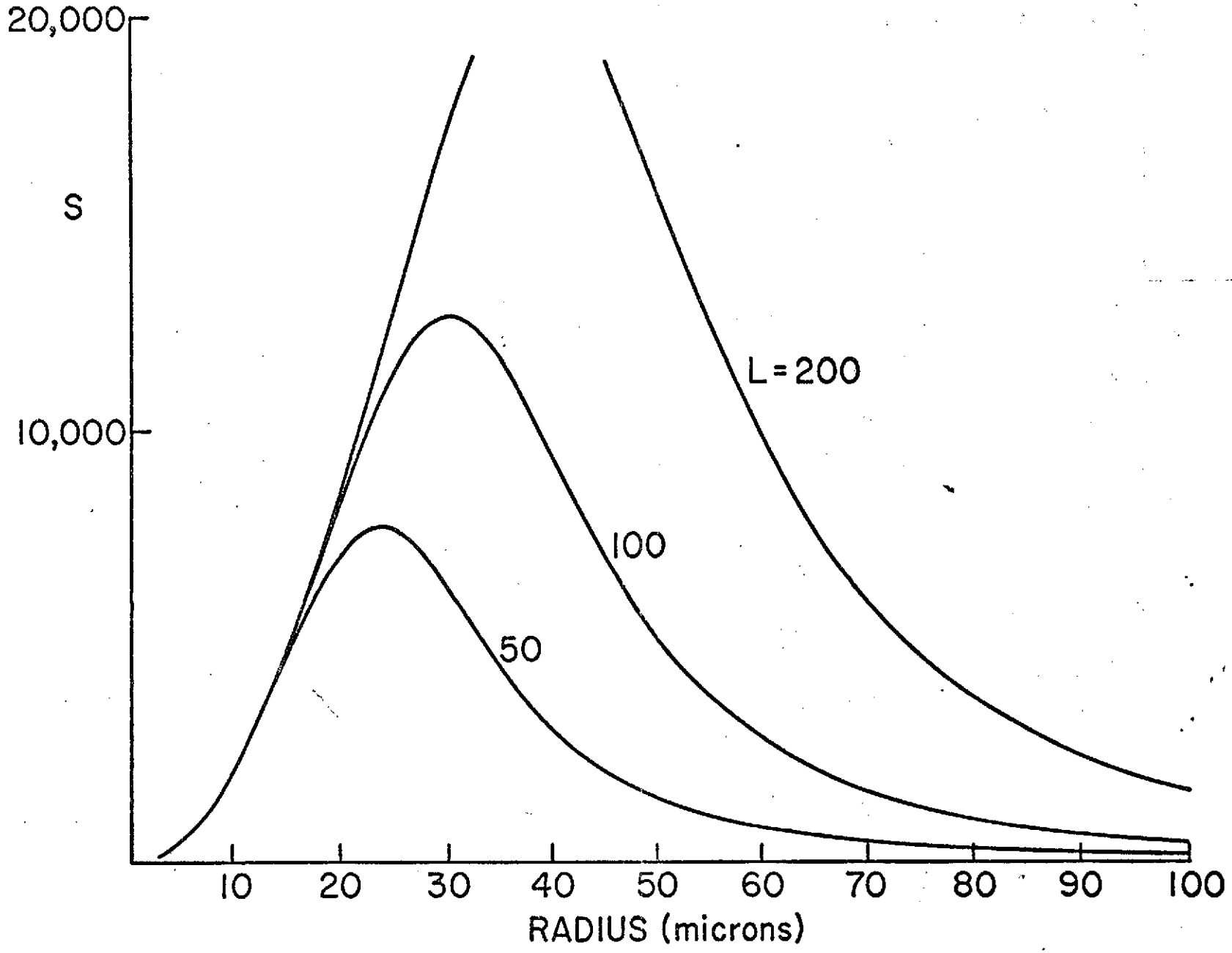

Figure 16
Shows how the p = 10 psi curve varies with column length.

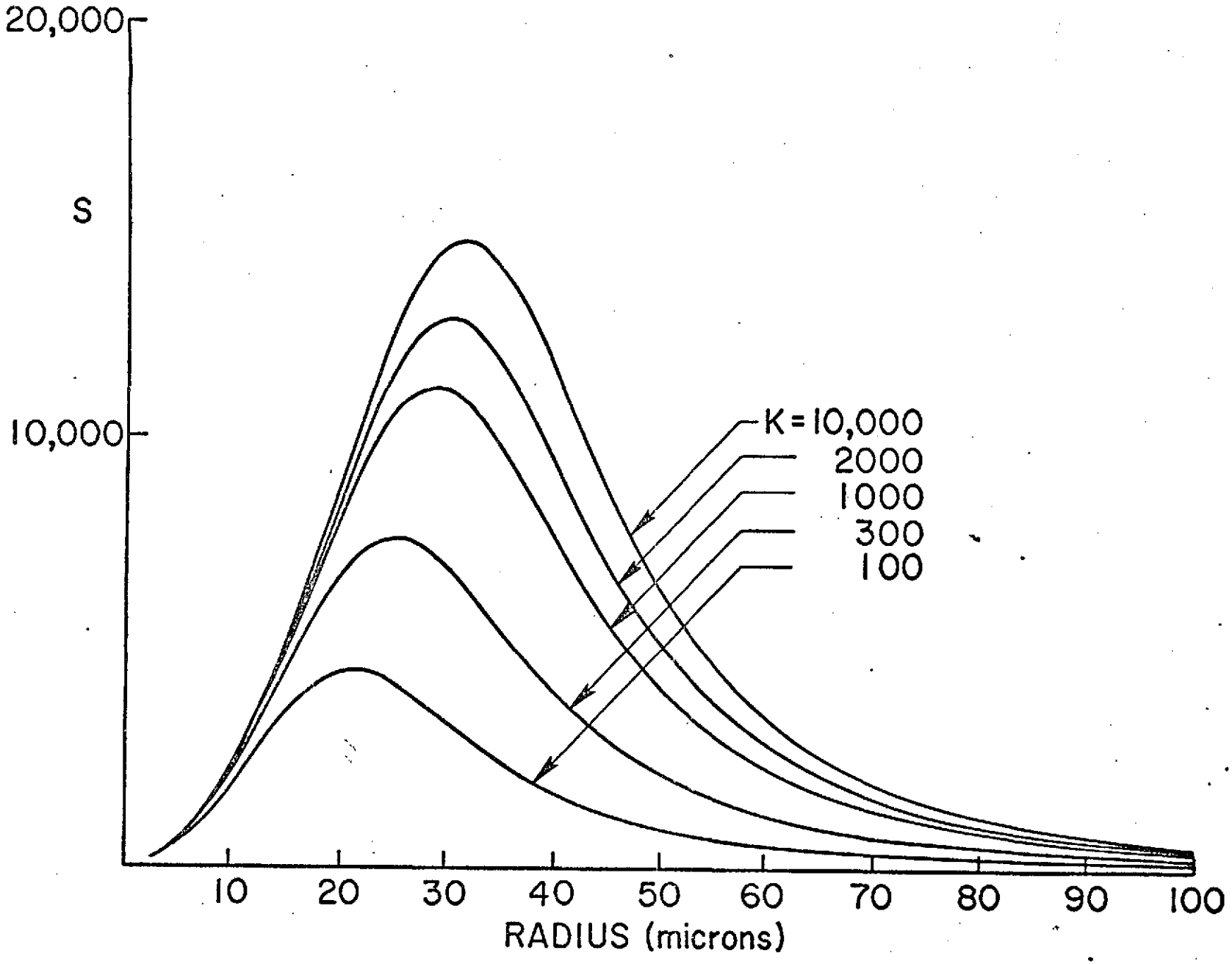

Figure 17
A plot separation with p = 10 and K as a parameter.

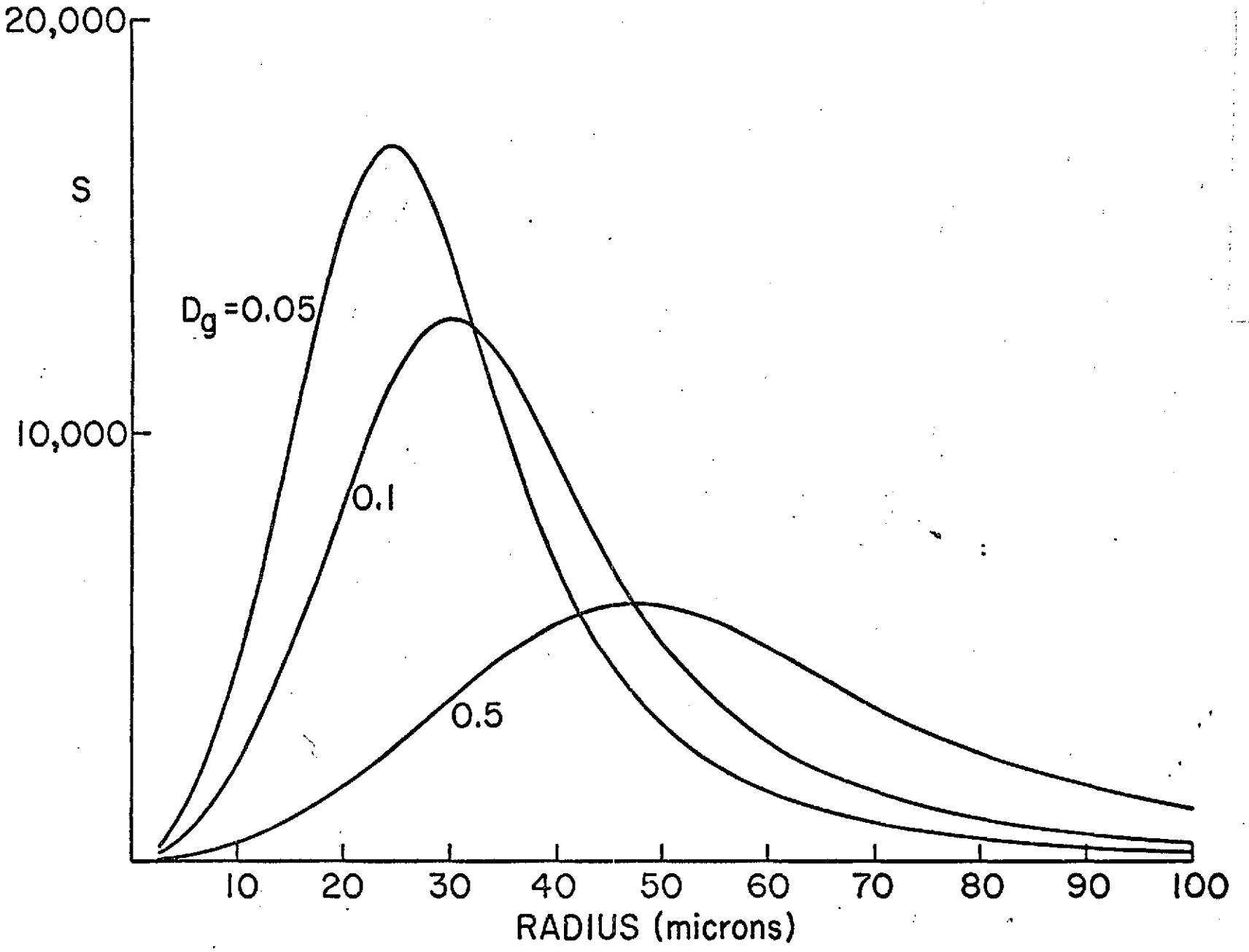

Figure 18

Separation versus capillary radius and different diffusion coefficients.

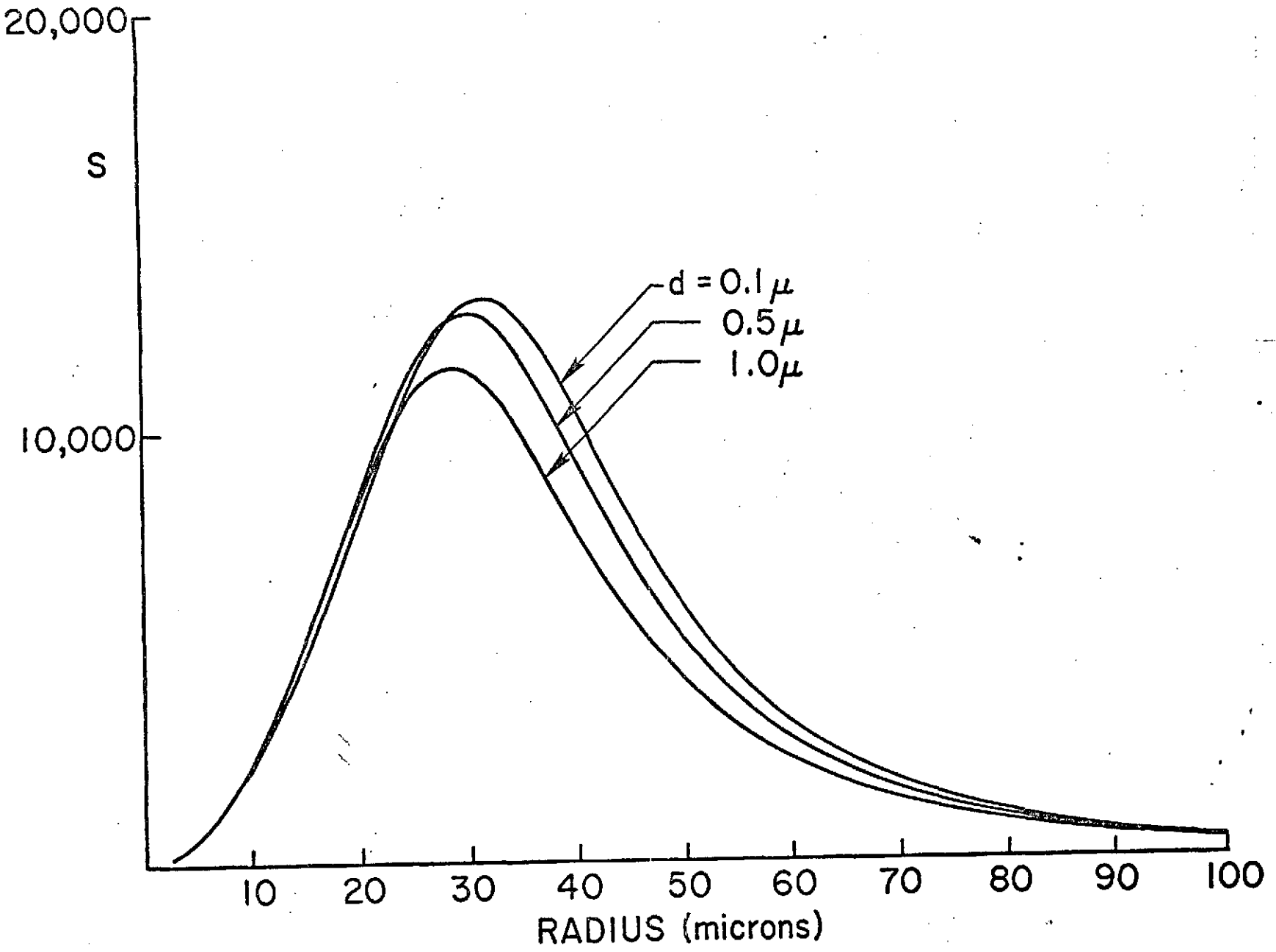

Figure 19

Separation versus capillary radius and different stationary layer thicknesses.

A second major problem facing the miniature GC system is that of sample size. As the column radius is decreased, the total weight of liquid phase in the column also decreases. Furthermore, for maximum separation, the liquid layer thickness d is made as small as possible, again resulting in decreased weight of liquid phase. But as the amount of stationary phase is decreased, the maximum allowable sample also decreases. For the miniature column, this results in maximum gas sample volumes on the order of a nanoliter. Provided that the miniature injection system can even inject such small volumes, the thermal conductivity detector might not be able to detect the output peaks. The possibility of experimentally verifying the theoretical separation factor curves presented here for the miniature column, completely depends upon the success of the miniature TC detector.

IV. Column Lining

The thickness of the stationary phase liquid layer is of obvious importance in view of the direct linearity of plate height H with the effective thickness squared, d^2. Only in the most ideal case could the liquid distribution in the capillary column be of uniform thickness. The liquid phase in the column is subject to both adsorption and capillary forces. The intermolecular attraction between the solid surface and the liquid leads to adsorption of a uniform layer of liquid on the column wall. The liquid-liquid molecular attraction, responsible for surface tension, leads to capillary condensation in pores on the wall. The liquid phase in surface pores, collected by capillary forces, is in equilibrium with a distributed layer of only 50Å thickness. Thus, any initial uniform layer greater than 50Å thick will pool itself in the irregularities of the column wall. This results in the layer thickness d varying from almost nothing to several microns in the surface pores. The best situation occurs when the surface has a uniform distribution of pores approximately 1μ in diameter. In this case the small pores serve to hold the liquid and prevent it from forming large droplets.

In the miniature column, this problem is enhanced in two respects. Since the spiral groove is silicon and the cover plate is glass, the two halves of the column cross section have different surface characterisitcs. This could lead to gross maldistribution of the liquid phase resulting in poor column efficiency. Also, capillary forces tend to draw the liquid into areas of reduced radius of curvature. This leads to the formation of fillets of liquid along the sharp junction of the cover plate and silicon wafer. Both of these problems might be reduced by proper etching and shaping of the silicon and glass surfaces.

V. Miniature Conductivity Detectors

Two different approaches toward fabricating a miniature thermistor-type detector were explored, in order to determine the most suitable detector for a miniature gas chromatograph.

First, an attempt was made to fabricate a miniature flake thermistor of the order of 250 μm square by 50 μm thick with zero power resistance of the order of 20 Kilohms. Large thermistor wafers ($1\frac{1}{2}$ X 5 X .012 inch) were obtained

from Gulton Industries, Metuchen, New Jersey, in various types of thermistor material. We eventually used the "Type E" material for fabrication experiments.

Gold was evaporated onto the coarse, granular surface of the thermistor wafer. Because of the coarseness, we found it preferable to evaporate a double layer of gold, each layer evaporated in a different direction, in order to make good bonding pads. Using an appropriate mask and a photoresist process, gold was removed from most of the wafer, leaving only an array of bonding pads. The photoresist exposure was costly in terms of yield, because of the warped surface of the thermistor wafer; the larger pieces of wafer suffered extensive fragmentation during exposure, due to the mask-to-wafer pressure in the exposure setup.

After the bonding pads were formed, the backside of the thermistor wafer was etched using HCl at 42 °C, to reduce the thickness from 320 μm to 50 μm. The thin wafers were then scribed in order to obtain individual thermistors. 25 μm gold wires were then attached to individual thermistor chips using conductive epoxy, and the finished flake thermistor was mounted in a standard transistor header. A typical resistance-vs.-current characteristic of one of the thermistors is shown in figure 20.

We conclude that it is certainly possible to fabricate a miniature thermistor via this procedure, but is is probably impractical. In particular, it would be necessary to find a material whose mechanical properties (particularly smoothness) permit a more precise definition of the required small dimensions.

The second exploration concerned the use of a high-resistivity silicon as a basic thermistor material. Figures 21-24 show calculated resistivity and percentage change in resistivity versus temperature for silicon doped with 10^{13} and 10^{12} impurity atoms per cm^3. Quite apparently, the more lightly doped silicon will serve very well as a thermistor in a temperature range around 100 °C. This material has a room-temperture resistivity of approximately 10,000 ohm cm. Sample quantities of silicon with this resistivity have been obtained; it is planned that small thermistors will be fabricated using beam leads for connections, in the near future.

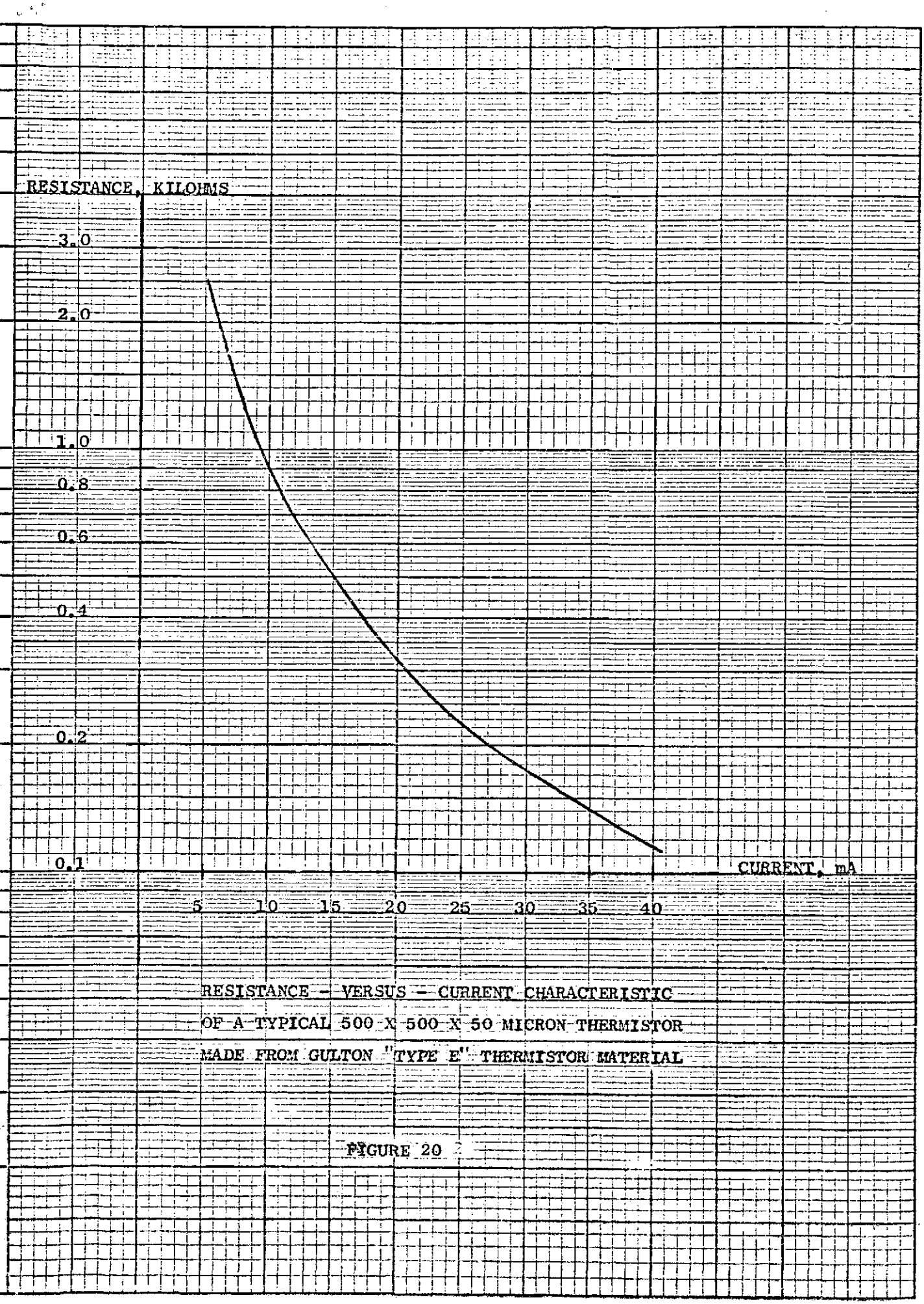

RESISTANCE - VERSUS - CURRENT CHARACTERISTIC
OF A TYPICAL 500 X 500 X 50 MICRON THERMISTOR
MADE FROM GULTON "TYPE E" THERMISTOR MATERIAL

FIGURE 20

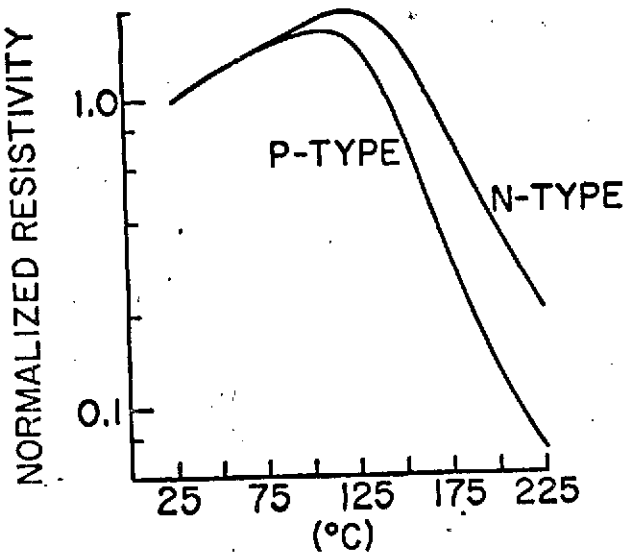

Figure 21 "Normalized Resistivity" vs. temperature for silicon with doping levels of 10^{13}.

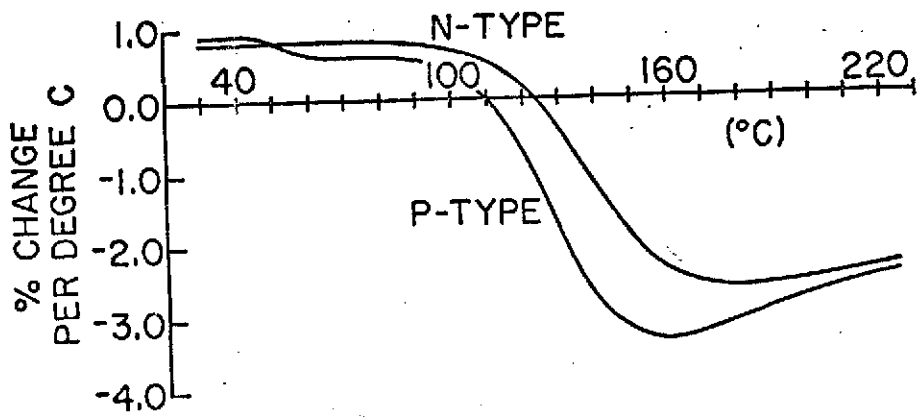

Figure 22 "Alpha" versus temperature for silicon with doping levels of 10^{13}.

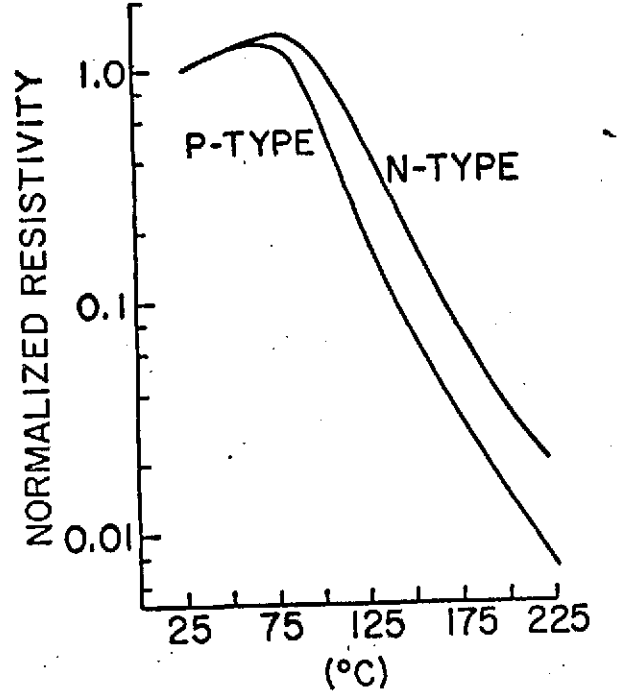

Figure 23 "Normalized Resistivity" versus temperature for silicon with doping levels of 10^{12}.

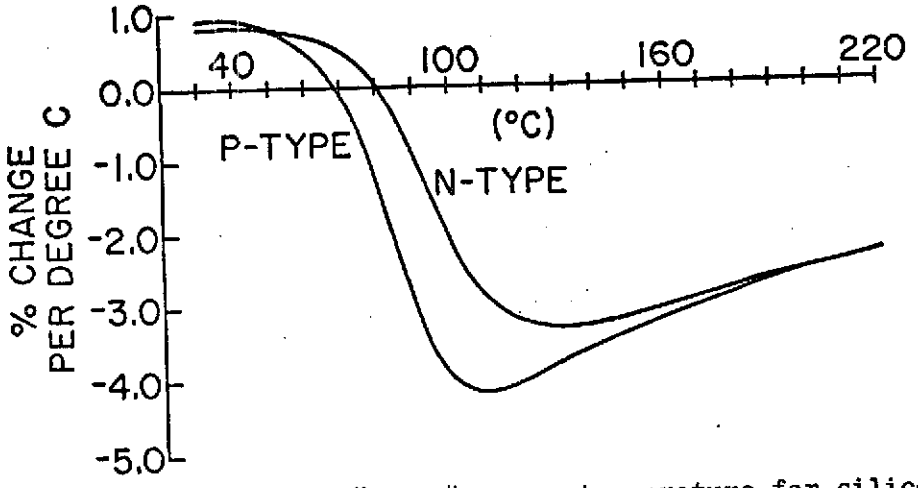

Figure 24 "Alpha" versus temperature for silicon with doping levels of 10^{12}.

Solid State Accelerometer*

A project has been established to develop a silicon accelerometer based on a strain-sensitive piezoresistor in a cantilevered silicon beam. Figure A1 is a photograph of the first sensor specifically designed for this function. The straight, narrow region in the middle of the sensor is a U-shaped diffused resistor that is strain sensitive. In the broad, left-end of the sensor is a second resistor of the same length as the resistor in the arm; this second resistor is intended to serve as a reference resistor for temperature compensation. The accelerometer is attached to its mount via this broad region containing the reference resistor. At the right end of the accelerometer is a widened region to which a mass can be attached by epoxy glue. The mounted structure will eventually be housed in a small container which includes a viscous fluid which will provide critical mechanical damping to the beam and mass.

Substantial progress has been made in fabricating a transducer specifically designed for use as an accelerometer. Some problems have been encountered, however, which, until resolved, will limit our ability to batch fabricate the transducers. How closely the sensitivities of the transducers can be matched is another question still to be answered.

A first-order analysis of the factors governing transducer sensitivity was made prior to the design of the current model. Both the mechanics of the cantilevered structure and the factors governing the piezoresistivity of silicon were considered, and further analysis will be attempted when a larger background in statics and fluid mechanics has been acquired. The latter should be of use in considering damping the structure via a viscous liquid inside the case. The earliest devices we made suggest that a resonant frequency of the order of one kilohertz and a Q of several thousand can be expected. Thus it might be desirable to damp the structure and eliminate problems associated with excitation of the resonant frequency.

Analysis showed that the primary factors governing the sensitivity of the device are the length of the beam, $1/(\text{thickness})^2$, $1/(\text{width})$, the weight attached to the end of the beam, and π_{44}, which is inversely proportional to the resistivity of the silicon used to make the resistors. These factors were used in designing the masks and processing schedule to produce devices with sensitivity comparable to the original accelerometer we produced. Mastering the various integrated circuit processing skills involved and producing the transducers presented no problems except in the final step (before packaging the transducers). The process calls for separation of the transducers from the silicon wafer by etching from the back side. Each transducer is surrounded by an etched area about 50 microns deep, so that the transducers should be 50 microns thick at the time of separation. The first attempts were unsuccessful. The etch did not etch parallel to the back surface, but rather at an angle severe enough that some transducers disappeared (destroyed by the etch) before others were separated. After some consideration of the problems a different etch, which was reported to produce very good results over large areas, was tried. This time the etching procedure worked beautifully. All 24 transducers separated nearly simultaneously, and none was lost due to non-uniformity of the etch.

*This work is being supported by the Joint Services Electronics Program under grant No. N000-14-67-A-0112-0004 JSEP. It is reported here for informational purposes only.

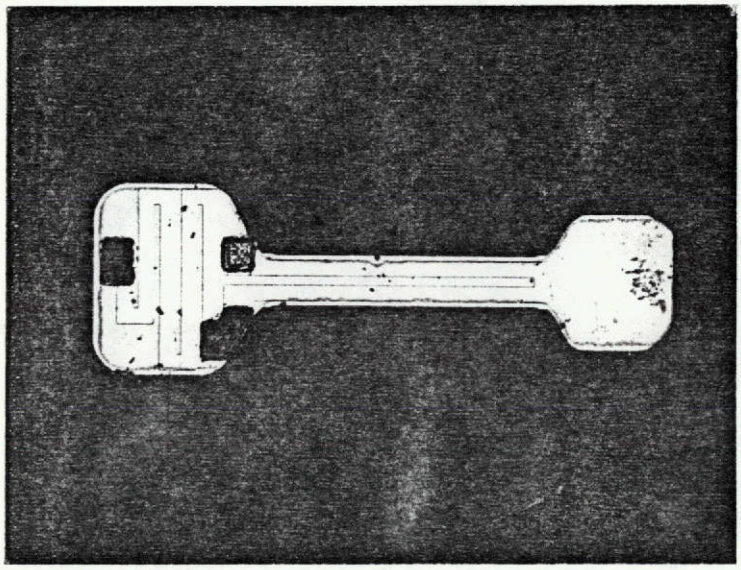

2.1 mm

It has not yet been possible to mount any of the transducers produced using the second etching procedure. However, three transducers were salvaged from the initial attempts at the separation etch, and two of these were mounted on TO-5 headers using a conducting epoxy. Leads were attached to one using a thermocompression bonder. Bonding each lead to the transducer took several attempts, and one try resulted in cracking the silicon, apparently because the epoxy did not provide a firm enough base for the chip. This problem can probably be eliminated with the use of solder squares specifically designed for mounting chips on headers. The improved thermal contact may also make bonding to the chip easier.

Once more transducers have been mounted a careful study of their sensitivity will be made, including an effort to check, in so far as now possible, the validity of the linear model used to predict the dependence of sensitivity on various parameters. Any problems encountered in mounting and use will be analyzed and their solutions incorporated in a new design. Changes in the process schedule will also be made where necessary to produce desired resistivities, beam length and thickness, etc.